Baseline adjustment scheme
for near- and far-fault records

R. Rupakhety, S. U. Sigurðsson & R. Sigbjörnsson
Earthquake Engineering Research Centre (EERC), University of Iceland

15 WCEE
LISBOA 2012

SUMMARY:
High quality digital strong-motion accelerographs have opened up the possibility of extracting ground motion characteristics at much lower frequencies than offered by analog instruments. This paper focuses on a baseline adjustment scheme which reduces noise-induced distortion of ground-motion accelerometric signals, and unlike high-pass filtering, retains potentially useful information at long periods. The criteria used to establish the methodology is based on the shape of earthquake Fourier spectra at low frequencies, leading to an objective and simple selection of parameters. Estimation of co-seismic deformation in near-fault zones is achieved and no limits are set to the use of response spectra ordinates at long periods. Case studies from recent earthquakes show that the proposed technique can be used effectively to adjust for baseline shifts in high quality accelerometric data and can be used on records from the near-fault as well as the far-fault regions.

Keywords: Baseline adjustment, Baseline correction, permanent displacement, long-period motion

1. INTRODUCTION

Processing of accelerometric strong-motion records is essential to remove noise contaminating the recorded signal. The effects of noise contamination, albeit of small amplitude and barely distinguished in recorded ground acceleration, is often manifested as clearly visible distortion of derived time series and quantities such as velocity and displacement waveforms as well as long-period response spectrum amplitudes. This reduces the confidence in estimating important ground-motion parameters — such as peak ground velocity (PGV), peak ground displacement (PGD), permanent ground displacement in the near-fault zone and long-period spectral ordinates — for engineering applications.

Permanent displacements and low-frequency motion can be accurately obtained from accelerometric data only if six components of ground motion (three translational and three rotational) are recorded (Grazier, 2006). It has been common practice to integrate individual translational acceleration time series to obtain corresponding ground velocity time series, which are further integrated to estimate ground displacement time series. With only translational components of acceleration available, velocities and displacements computed by integration from acceleration series are often assessed as uncertain. Inaccuracies in velocities and displacements so obtained can be attributed to a number of reasons. In the near-fault region, the movement of the instrument's base is not purely translational and the recorded signal, in many cases, contains instrument response to rotational components of ground motion. These effects are known as tilts. Apart from tilts, digitized as well as digitally recorded accelerograms are contaminated by complicated shifts of zero acceleration level, commonly known as the baseline. Baseline shifts are small but instantaneous offsets in acceleration zero-level. Although they are hardly visible in acceleration series, they tend to amplify through the integration process resulting in significant drifts in the integrated velocity and even more clearly seen in displacement time series, where they appear as linear and quadratic trends, respectively.

Traditional methods in strong-motion data processing have relied on band-pass filtering. While filtering of low-frequency noise is often desirable to reduce the distortion of displacement and velocity waveforms, application of crude filtering can lead to the loss of long-period components of earthquake

ground motion. High-pass filtering does not implicitly establish a realistic baseline towards the end of the velocity and displacement traces, and a pre-event drift is often present. A visual linear trend is typically identified in the velocity trace before filtering, resulting in a non-zero velocity at the end of the record. Similarly a polynomial trend becomes apparent in the displacement trace, rather than reaching a stable value towards the end. Although these trends can be diminished or even removed by applying the traditional filtering (higher cut-off frequency), a significant information from the actual signal can be inadvertently lost in the process. An example of the effects of the choice of filter parameters is visualized in Fig. 1.
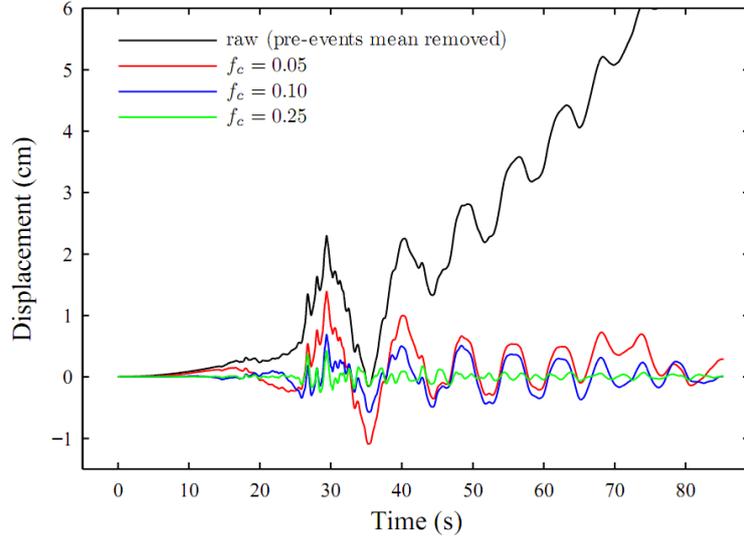

Figure 1. Displacement trace derived from the accelerogram at LTZ-station recording the 2011 M_w 6.3 Christchurch earthquake at an epicentral distance of 95 km. Results obtained from the unfiltered data is indicated by the black curve, while the other curves correspond to filtered data. A 4th order high-pass acausal Butterworth filter is used with cut-off frequencies (f_c) as indicated in the figure legend. Note the sensitivity of peak ground displacement to the choice of f_c.

To avoid such influences and yet obtain acceptable velocity and displacement waveforms, baseline adjustment techniques are a potential replacement for high-pass filtering. Long-period contamination of digital records is often a result of baseline distortion — small and random offsets of the zero level of the accelerogram, possibly a form of signal generated noise hardly visible in the acceleration record, but amplified as unrealistic trends in the integrated velocity and displacement waveforms. Iwan et al. (1985) introduced a simple two-stepped noise model of baseline variation based on the idea of mechanical and/or electrical hysteresis within the digital instrument's transducer during the recording of a strong-ground motion. In this paper, we present a baseline adjustment scheme based on the noise model of Iwan et al. (1985) which efficiently reduces noise-induced distortion of ground-motion signals, and unlike high-pass filtering, retains potentially useful information at long periods.

2. BASELINE ADJUSTMENT SCHEME

2.1 The noise model

An illustration of the two stepped noise model and the parameters used to quantify the baseline shifts can be seen in Fig. 2. The baseline adjustment procedure is based on the assumption that variations in acceleration baseline are confined between time instances t_1 and t_2. The baseline shift in acceleration is modelled as shown with the thick blue line in Fig. 2. This shift is added to the pre-event-mean removed acceleration. Then the artificially contaminated acceleration is integrated to obtain velocity, shown with the red line. The black line corresponds to the integral of shift in acceleration baseline. Obviously the linear trend in velocity due to baseline shift is caused by the slope of the black line after t_2. Iwan et al. (1985) proposed that baseline shifts occur during the strong shaking and can be modelled

as two offsets. The first offset a_m represents an average of several complicated shifts between t_1 and t_2. A second offset a_f is assumed to occur at t_2. If we assume this model to be correct, then baseline adjustment can be performed in a very straight forward way. A straight line is fitted to the linear trend in velocity, and its slope gives the value of a_f. In practice, the linear trend might not be obvious right after t_2, in which case linear fitting in velocity is done between time points t_3 and t_{end}, where t_3 is chosen well after strong motion has subsided, and t_{end} is the end of the record. The fitted line is then extrapolated to t_2.
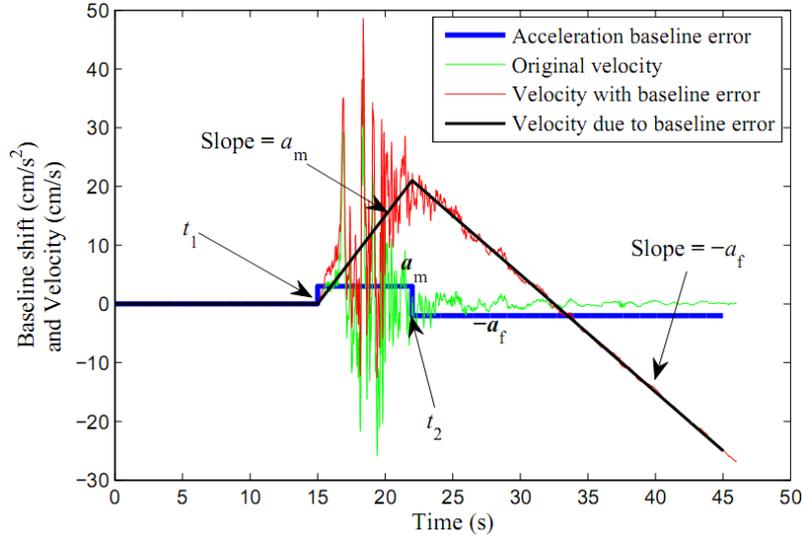

Figure 2. Illustration of baseline shifts in acceleration and the corresponding linear trend in integrated velocity. The green line corresponds to the velocity obtained by integrating an acceleration record (pre-event mean removed) from the 2008 Ölfus earthquake. Baseline shifts equal to a_m and $-a_f$ added to the acceleration record are shown with the thick blue line. The black line corresponds to the integral of baseline shift and the red line corresponds to the velocity obtained by integrating the acceleration record contaminated with the artificial baseline shifts.

Several baseline adjustment schemes have been published in the literature based on the above model. This includes the work of Iwan et al. (1985), Anderson et al. (1986), Boore (2001), Boore et al. (2002), Wang et al. (2003), Wu and Wu (2007) and Akkar and Boore (2009). Although the method is simple, selections of t_1, t_2 and t_3 are arbitrary, and researchers have proposed different schemes for selecting these parameters. A thorough investigation of these models and their sensitivity to the selection of parameters can be found in Rupakhety (2010) and Rupakhety et al. (2010a).

2.2 The proposed scheme

The baseline adjustment scheme introduced here is primarily based on the noise model proposed by Iwan et al. (1985) and the assumption, proposed by Wu and Wu (2007), that the corrected displacement resembles a ramp step function in the near-fault zone where permanent displacement is expected to occur. This assumption is further rationalised and extended to far-fault records by the use of the properties of the theoretical source spectra originally proposed by Brune (1970, 1971).

The time instance t_1 can be automatically selected as the instance when the recorded acceleration exceeds a certain threshold and the first adjustment of baseline offset is applied at this instant. The parameter t_3 is chosen as the time instance when the strong ground motion has expired. This quantity can be automatically selected as the instance when the Arias-Intensity derived from the acceleration series has reached a certain threshold. The time instance to apply the second adjustment t_2 is somewhere in the range between t_1 and t_3 and can be selected using the criteria described in the following.

If it is assumed that in the near-fault zone the displacement waveform $D(t)$ is a perfect ramp step function:

$$D(t) = \begin{cases} 0 & t < t_1 \\ H(t - t_1) & t_1 \le t \le t_3 \\ HT & t > t_3 \end{cases} \tag{2.1}$$

Then the corresponding velocity $V(t)$ becomes a boxcar given as

$$V(t) = \begin{cases} H & \text{for } t_1 \le t \le t_3 \\ 0 & \text{elsewhere} \end{cases} \tag{2.2}$$

where

$$t_1 = c - \frac{T}{2} \tag{2.3}$$

$$t_3 = c + \frac{T}{2} \tag{2.4}$$

Here, T denotes the duration between the time points t_1 and t_3 and c their average, i.e. the boxcar is centred at time c, further more, it has the height H, i.e. constant velocity. The displacement and the corresponding velocity model are shown in Fig. 3.
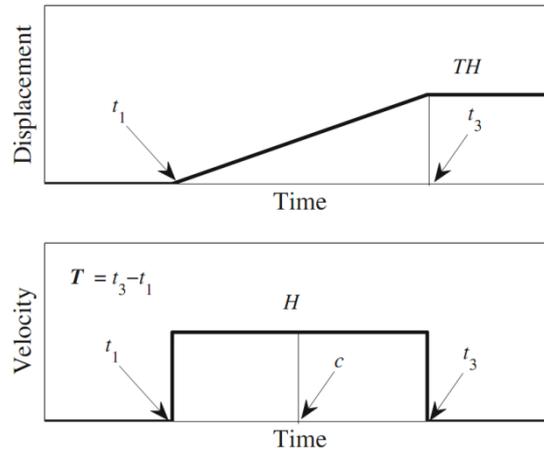

Figure 3. Displacement modelled as a ramp (top) and the corresponding velocity (bottom), which is a boxcar of width T and centred at c. The displacement starts at t_1 and reaches a maximum value of TH at time t_3 after which it remains constant. The slope of the ramp is equal to the height of the boxcar.

The Fourier amplitude spectra (FAS) of the boxcar velocity is then evaluated. If f is the frequency then the Fourier transform of velocity is given by

$$F(f) = H e^{-i2\pi f c} \frac{\sin(\pi f T)}{\pi f} \tag{2.5}$$

and hence the FAS is given by

$$FAS_v(f) = |F(f)| = HT \left| \frac{\sin(\pi f T)}{\pi f T} \right| \tag{2.6}$$

The Fourier amplitude of velocity at zero frequency can be computed by taking the limit on Eqn. (2.6) as $f \to 0$, which gives

$$FAS_v(0) = \lim_{f \to 0} HT \left| \frac{\sin(\pi f T)}{\pi f T} \right| = HT \tag{2.7}$$

From Eqns. (2.6) and (2.7) it is clear that the FAS of velocity for a displacement modelled as a ramp approaches the permanent displacement at low frequencies and decays as f^{-1} above the corner frequency. If additional extremely long-period noise is not present in the signal, and if there are no baseline offsets, the FAS of velocity should approach the permanent ground displacement asymptotically as the frequency approaches zero. In addition, the FAS of the corrected velocity should be flat at low frequencies.

Investigation of Fourier amplitude spectra of earthquake ground motion records obtained at the near- and the far-fault area reveal that the Brune source spectra (Brune 1970, 1971) based on a circular fault model provides a reasonable estimate of the spectral content of ground motion. This has, among other things, revealed that the low-frequency amplitude of the far-fault displacement spectra is proportional to the energy released in an earthquake event — from which it follows with the consideration of finite energy release, that the Fourier displacement amplitude spectrum is flat at low frequencies. If, on the other hand, permanent static displacement of the ground occurs, a simple ramp model of ground displacement follows that the low-frequency asymptote of the Fourier velocity spectrum approaches the permanent ground displacement (see above). These observations are also apparent from the Brune source spectra — the far-fault displacement spectrum is given as (Brune 1970, 1971)

$$\left| D(\omega) \right| = \bar{R}_{\theta\phi} \frac{\sigma \beta}{\mu} \frac{r}{R} \frac{1}{\omega^2 + \omega_c^2} \tag{2.8}$$

and the near-fault displacement spectrum as

$$\left| D(\omega) \right| = \frac{\sigma \beta}{\mu} \frac{1}{\omega \sqrt{\omega^2 + \tau^{-2}}} \tag{2.9}$$

Here, ω is the circular frequency in rad/s ($\omega = 2\pi f$ where f is the frequency in Hz), $\bar{R}_{\theta\phi}$ is the root-mean-square average of the radiation pattern, σ is the stress-drop, β is the shear-wave velocity, μ is the rigidity of the crust, r is the radius of the fault, R is the source-to-site distance, ω_c is the corner frequency, and τ represents the rise-time.

The theoretical far-fault displacement and near-fault velocity spectra are shown with blue curves in Fig 4, on the left and the right graphs respectively, along with their Fourier amplitude spectrum (FAS) counterparts obtained from two records of the 2008 Ölfus earthquake. As seen in the figure (left), the low-frequency portion of the theoretical far-fault displacement-spectra is relatively flat which becomes apparent when both axes are in logarithmic scale. Presence of long-period noise causes the displacement spectra to exhibit a small trend at low frequencies, thus a deviation from the horizontal asymptote of the theoretical model. The results plotted in Fig 4 correspond to the baseline adjusted acceleration data which reveal that the long-period distortion has been effectively reduced. This provides an objective criterion of constraining the baseline adjustment operation on far-fault accelerograms — maximizing the flatness of the displacement Fourier amplitude at low frequencies. For near-fault data, this criterion translates to maximizing the flatness of the velocity Fourier spectrum at low frequencies.
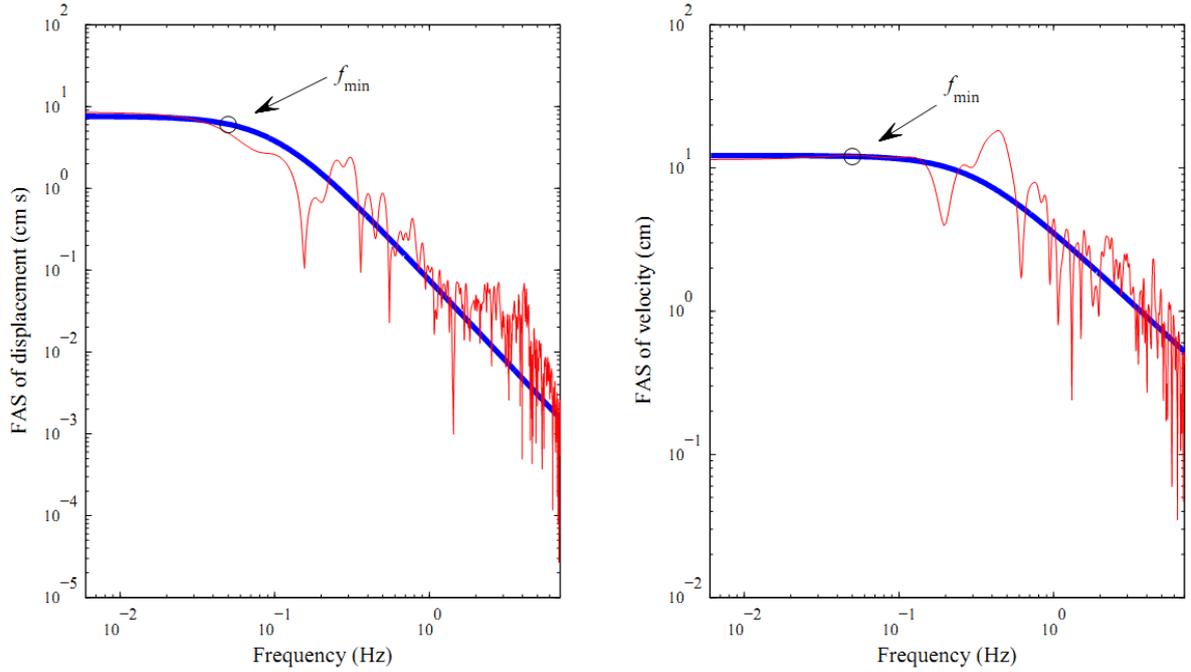
Figure 4. Fourier amplitude spectra (FAS) of two records from the May 2008 M_w 6.3 Ölfus earthquake. *Left:* Displacement-FAS of Hella-record at an epicentral distance of 36 km (red curve) and the corresponding Brune far-fault spectrum (blue curve). *Right:* Velocity-FAS of Selfoss-Hospital-record at an epicentral distance of 8 km (red curve) and the corresponding Brune near-fault spectrum (blue curve). The records have been processed by the procedure proposed in the present paper.

The frequency defining the upper limit of the low frequency phase (the flat asymptotic part in Fig. 4) is denoted as f_{min}. Before applying the baseline adjustment procedure, f_{min} needs to be determined. The value of f_{min} should be lower than the earthquakes corner frequency, which can be estimated by a method based on spectral moments (Ólafsson 1999; Andrews 1986). The criterion used to objectively select the time instance t_2 where the second baseline adjustment is applied is to select the time instance that maximizes the flatness. The flatness is evaluated by calculating the flatness coefficient $-\phi-$ for the low frequency range $\left(f_0 \leq f \leq f_{min} \right)$ of the FAS as

$$\phi = \frac{|r|}{|b| \cdot \sigma} \tag{2.10}$$

where r, b, and σ are respectively the linear correlation coefficient, the slope, and the standard deviation of the displacement FAS in the frequency range defined above.

A detailed description of the adjustments schemes algorithm and its application can be found in Rupakhety (2010), Rupakhety et al. (2010a) and Sigurdsson et al. (2011).

3.   CASE STUDIES

In this section, examples of the baseline adjustment schemes efficiency are visualized. The recorded time series used are from three recent earthquakes: Ölfus Iceland 2008 (data available at www.isesd.hi.is), L'Aquila Italy 2009 (data available at itaca.mi.ingv.it) and Christchurch New Zealand 2011 (data available at www.geonet.org.nz).
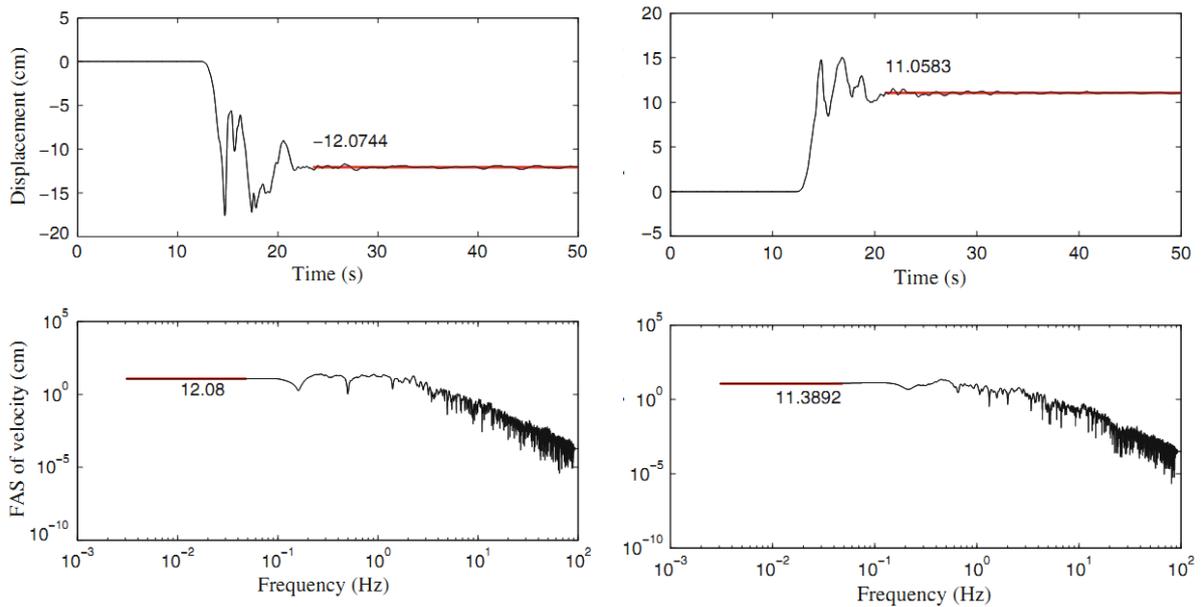
3.1   Near-fault

Figure 5. *Left*, Baseline adjusted displacement waveform and corresponding FAS of velocity for the north-south component recorded at Selfoss Town-Hall during the 2008 Ölfus Earthquake. Positive displacement is towards the north. *Right*, same as left but for the east-west component. Positive displacement is towards the east. Notice how the flat low frequency part of the FAS reaches a value close to the permanent displacement achieved (indicated by the red lines in the figure).
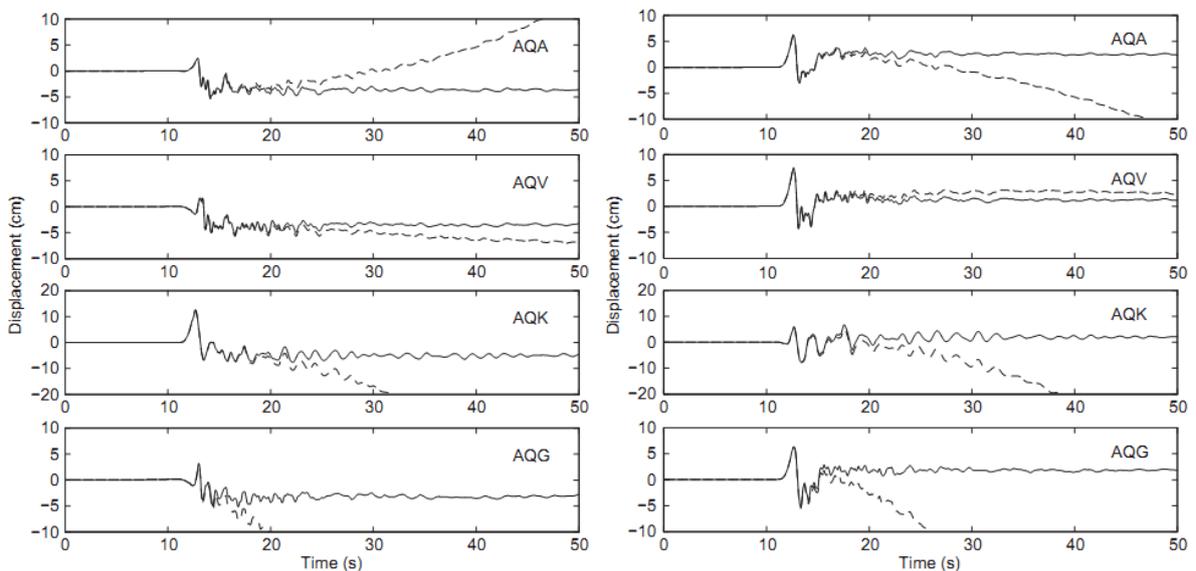

Figure 6. Displacement waveforms at AQA, AQV, AQK and AQG stations, recording the 2009 L'Aquila earthquake. The names of the stations are shown in each plot. *Left,* north-south components, positive towards the north. *Right*, east-west components, positive towards the east. The raw waveforms are indicated by a dashed line, while the baseline adjusted waveforms are plotted with a solid line.
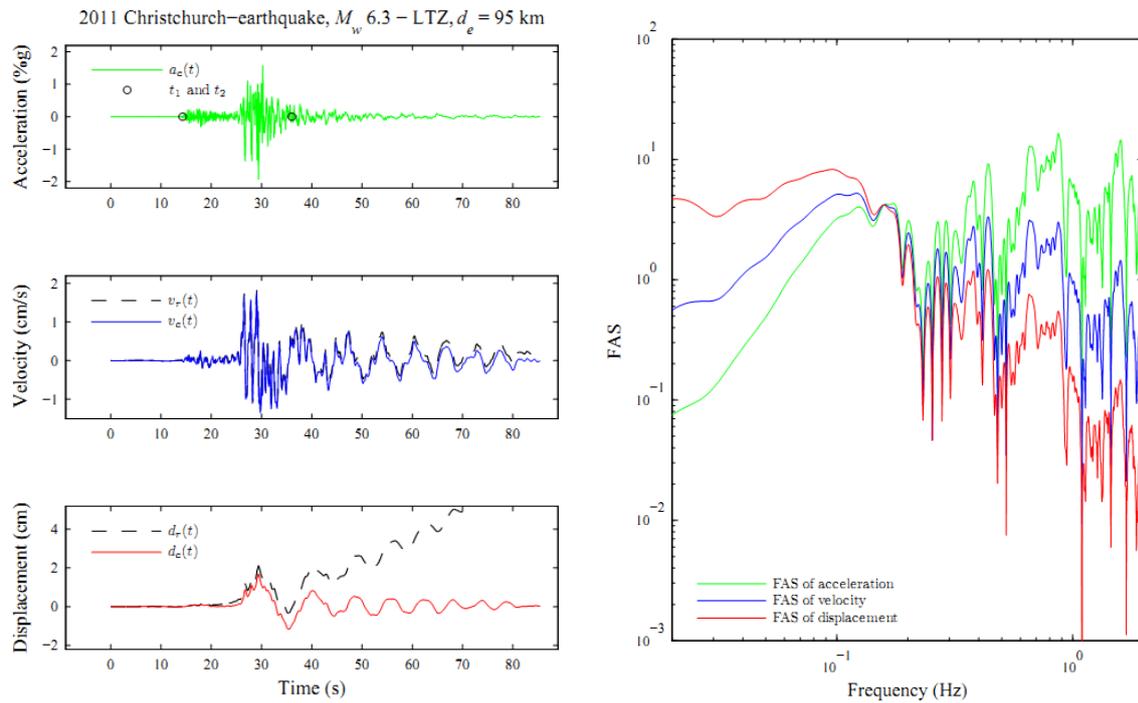
3.2 Far-fault

Figure 7. The East-component at LTZ-station recorded at the 2011 Christchurch earthquake. Acceleration, velocity and displacement traces *(left)* and corresponding Fourier amplitude spectra *(right)*. The raw waveforms are indicated by a dashed line while the baseline adjusted waveforms are plotted with a solid line. The displacement waveform is plotted for filtered data in Fig. 1.
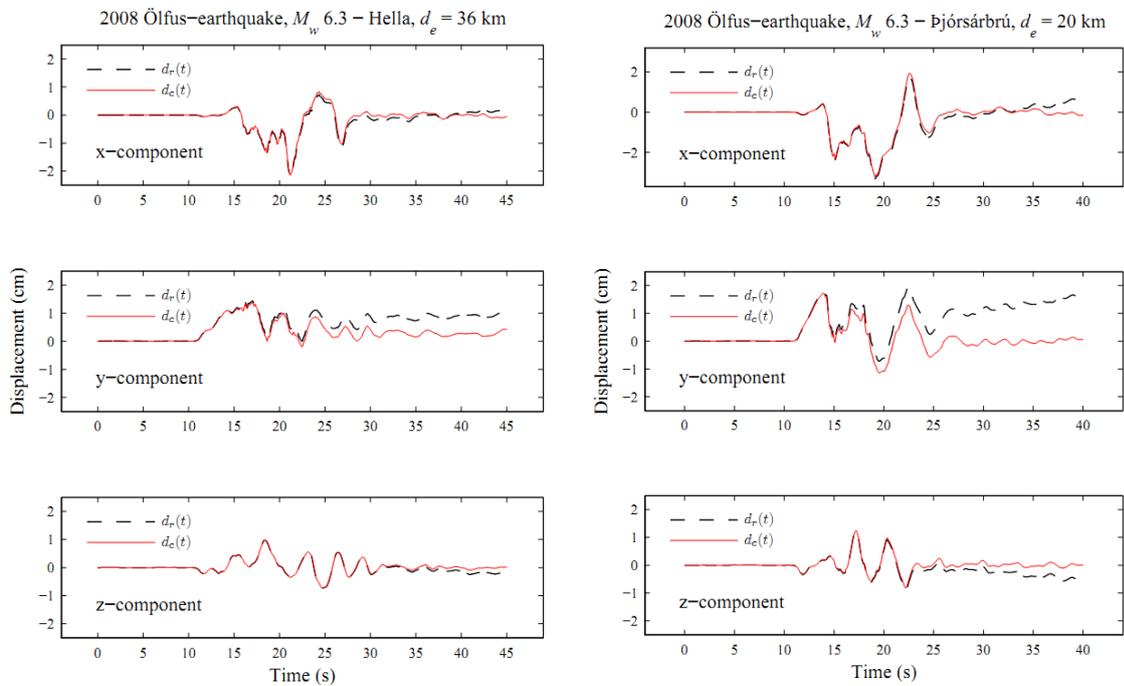

Figure 8. Baseline adjusted displacement waveforms of three components recorded at two sites during the 2008 Ölfus earthquake.

3.3   Response spectra

The maximum natural period is limited due to high-pass filtering — the cut-off frequency and the roll-off used in filter design being the controlling parameters. A potential advantage of using baseline adjustment is that, unlike high-pass filters, the processed data retain significant portion of long-period signal, thereby increasing maximum period up to which response spectral ordinates can be estimated. As an illustration, the average displacement response spectrum corresponding to 16 far-fault records of the 2011 Christchurch Earthquake is plotted in Fig. 9. The figure illustrates that results of the baseline adjustment procedure and high-pass filtering are quite similar at shorter natural periods. At periods close to and longer than the cut-off period ($1/f_c$), the baseline adjusted records exhibit higher spectral ordinates, indicating that the scheme retains long-period information which is inadvertently lost if filtering operations are employed.
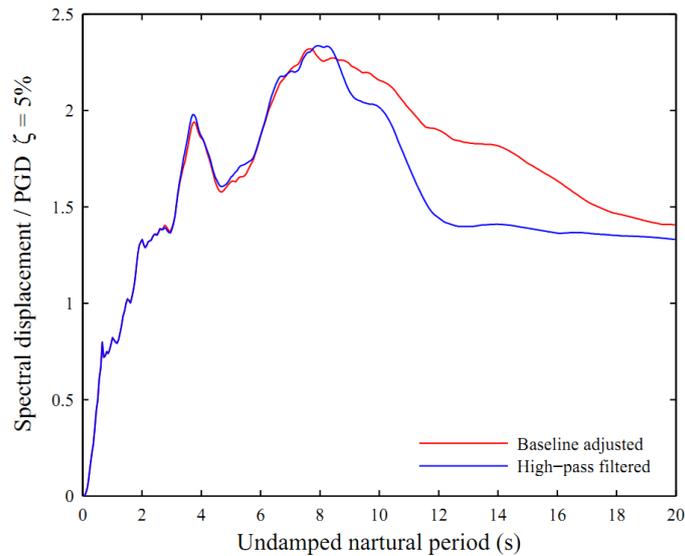

Figure 9. Average displacement response spectra of the East component of 16 far-fault records from the 2011 Christchurch Earthquake, epicentral distances: $30 \leq d_e \leq 100$. The spectra are normalised with corresponding PGD. The red line corresponds to a dataset that has been baseline-adjusted with the method proposed in this paper. The blue line corresponds to the same set but high-pass filtered using a 4th order acausal Butterworth filter with a cut-off frequency of 0.1 Hz (10s).

Another important observation from the same dataset is the difference in the peak values of ground displacement (PGD). The values obtained after baseline adjustment are on average 40% higher than those obtained from the filtered data.

4.   CONCLUSION

Long-period noise contamination in digital strong motion data poses difficulties in retrieving long-period motion and co-seismic deformations from near-fault stations. The baseline adjustment scheme proposed in this paper is an iterative automated process based on theory of earthquake source spectra. The criterion used to objectively constrain the procedure is the flatness of Fourier amplitude spectra at low frequencies. Based on the results obtained by processing a large number of digital records from earthquakes of different magnitudes, it is found that the proposed method has the advantages of producing results including stable displacement and velocity waveforms and retaining significant portion of long-period signal which is inadvertently lost by high-pass filtering techniques. This method is found appropriate for high-quality digital records where the amplitude of the strong-motion is of structural engineering interest.

REFERENCES

Anderson, J. G., Bodin, P., Brune, J. N., Prince, J., Singh, S. K., Quaas, R. and Onate, M. (1986). Strong Ground Motion from the Michoacan, Mexico, Earthquake. *Science (New York, NY)*, **233:4768**, 1043.

Andrews, D. J. (1986). Objective determination of source parameters and similarity of earthquakes of different size. *Earthquake source mechanics*, **37**, 259–267.

Akkar, S. and Boore, D. M. (2009). On Baseline Corrections and Uncertainty in Response Spectra for Baseline Variations Commonly Encountered in Digital Accelerograph Records. *Bulletin of the Seismological Society of America*, **99:3**, 1671.

Boore, D. M., Stephens, C. D. and Joyner, W. B. (2002). Comments on baseline correction of digital strong-motion data: examples from the 1999 Hector Mine, California, earthquake. *Bulletin of the Seismological Society of America*, **92:4**, 1543.

Brune, J. N. (1970). Tectonic Stress and the Spectra of Seismic Shear Waves from Earthquakes. *Journal of Geophysical Research*, **75:26**, 4997-5009.

Brune, J. N. (1971). Correction (to Brune, 1970). *Journal of Geophysical Research*, **76:20**, 5002.

Grazier, V.M. (2006). Tilts in strong ground motion. *Bulletin of the Seismological Society of America* **96:6**, 2090-2102.

Iwan, W. D., Moser M. A. and Peng, C. Y. (1985). Some observations on strong-motion earthquake measurement using a digital accelerograph. *Bulletin of the Seismological Society of America* **75:5**, 1225.

Ólafsson, S. (1999). Estimation of earthquake-induced response, PhD Thesis, Department of Structural Engineering, Norwegian University of Science and Technology.

Sigurdsson, S. U., Rupakhety, R. and Sigbjörnsson, R. (2011). Adjustments for baseline shifts in far-fault strong-motion data: An alternative scheme to high-pass filtering. *Soil Dynamics and Earthquake Engineering* **31:12**, 1703-1710.

Rupakhety, R. (2010). Contemporary issues in earthquake engineering research: processing of accelerometric data, modelling of inelastic structural response, and quantification of near-fault effects, PhD Thesis, Faculty of Civil and Environmental Engineering, School of Engineering and Natural Sciences, University of Iceland.

Rupakhety, R., Halldorsson, B. and Sigbjörnsson, R. (2010a). Estimating coseismic deformations from near source strong motion records: methods and case studies. *Bulletin of Earthquake Engineering*, **8:4**, 787-811.

Rupakhety, R. and Sigbjörnsson, R. (2010b). A note on the L'Aquila earthquake of 6 April 2009: Permanent ground displacements obtained from strong-motion accelerograms. *Soil Dynamics and Earthquake Engineering*, **30:4**, 215–220.

Wang, G. Q., Boore, D. M., Igel, H. and Zhou, X. Y. (2003). Some observations on colocated and closely spaced strong ground-motion records of the 1999 Chi-Chi, Taiwan, earthquake. *Bulletin of the Seismological Society of America*, **93:2**, 674.

Wu, Y. M. and Wu, C. F. (2007). Approximate recovery of coseismic deformation from Taiwan strong-motion records. *Journal of Seismology*, **11:2**, 159–170.